

Phase diagram of a polydisperse soft-spheres model for liquids and colloids

L. A. Fernández,^{1,2} V. Martín-Mayor,^{1,2} and P. Verrocchio^{2,3}

¹*Departamento de Física Teórica I, Universidad Complutense, 28040 Madrid, Spain.*

²*Instituto de Biocomputación y Física de Sistemas Complejos (BIFI), Spain.*

³*Dipartimento di Fisica, Università di Trento and CRS, SOFT, INFM-CNR, 38050 Povo, Trento, Italy.*

(Dated: March 23, 2022)

The phase diagram of soft spheres with size dispersion has been studied by means of an optimized Monte Carlo algorithm which allows to equilibrate below the kinetic glass transition for all sizes distribution. The system ubiquitously undergoes a first order freezing transition. While for small size dispersion the frozen phase has a crystalline structure, large density inhomogeneities appear in the highly disperse systems. Studying the interplay between the equilibrium phase diagram and the kinetic glass transition, we argue that the experimentally found terminal polydispersity of colloids is a purely kinetic phenomenon.

PACS numbers: 64.60.Fr, 64.60.My, 66.20.+d

The equilibrium phase diagram of dense classical fluids is far from being fully understood, especially as regards the influence over the freezing transition of some disorder in the parameters of the interaction. While fluids made of identical atoms crystallize easily upon lowering the temperature or increasing the density, the fate of *polydisperse* systems (colloids, for instance), where the particle size σ is sampled from a probability distribution, $P(\sigma)$, is still a matter of debate.

On the theoretical side, the effect of size dispersion, measured by the quantity δ (the ratio among the standard deviation and the mean of $P(\sigma)$) over the phase diagram has been addressed mostly in the case of the hard-spheres model, which is meant to describe colloidal systems [1]. At least for small polydispersity, δ seems to be the only feature of $P(\sigma)$ that controls the physical results. Different theories predict conflicting scenarios in the region of large δ . The moment free-energy method [2] suggests phase separation between many different crystal phases, each one with a much narrower size dispersion than δ (a phenomenon termed *fractionation*). However, a density functional analysis [3] predicts the existence of a terminal polydispersity δ_t beyond which the formation of the crystal is thermodynamically suppressed. Numeric simulations of the hard sphere model find some agreement with both the fractionation [4, 5] and the terminal polydispersity [6] scenarios. As regards models with a soft potential (e.g. Lennard-Jones), which are more appropriate to describe liquids, no extensive study on the effects of polydispersity has been performed so far.

On the experimental side, crystallization of very viscous colloidal samples with $\delta > \delta_t \approx 0.12$ does not occur, even after months spent from the preparation [7]. Further evidence supporting the terminal polydispersity scenario comes from the finding of reentrant melting (crystal to fluid transition when increasing the density) on polydisperse colloids in confined geometry [8].

Yet, these experimental results do not necessarily reveal features of the phase diagram. Indeed, the processes

needed to keep the system in thermodynamic equilibrium often become exceedingly slow. Such processes are the nucleation of the solid within the fluid and the α -relaxation in the super-cooled fluid [9].

Here we obtain the *equilibrium* phase diagram of polydisperse soft-spheres in the (N, V, T) ensemble, aiming to describe both liquids and colloids. This is made possible by the combination of an optimized Monte Carlo (MC) method (which, unlike standard MC, equilibrates *below* the kinetic glass temperature) and a novel Finite-Size Scaling study of the fluid-solid coexistence line. At all δ , a first-order freezing transition separates the fluid phase from the low temperature solid. This rules out the thermodynamic origin of the terminal polydispersity scenario. However, we show that a Brownian dynamics will not find crystallization for $\delta > 0.12$, in quantitative agreement with colloids experiments [7]. Furthermore, depending on polydispersity the solid phase can be either a crystal or an inhomogeneous phase (hereafter I-phase). The freezing temperature shows a reentrant behavior when increasing δ . Interestingly, in the range $\delta \in [0.12, 0.38]$ the kinetic glass transition occurs for temperatures, T , and densities, ρ , in the stable fluid phase.

Specifically, in our simulations soft-spheres of radius σ_i and σ_j at distance r interact via the pair potential [30]

$$V_{ij}(r) = \left(\frac{\sigma_i + \sigma_j}{r} \right)^{12}. \quad (1)$$

The effect of T and ρ is encoded in the single thermodynamic parameter $\Gamma \equiv \rho T^{-1/4}$. Although (1) generalizes well known models for simple liquids [10], its scale-invariant form suggests that it could describe as well colloids, whose size is in the micrometer range. We consider a flat size distribution, constant in the range $[\sigma_{\min}, \sigma_{\max}]$. In order to eliminate sample-to-sample fluctuations we follow [11], which for a flat distribution amounts to pick $\sigma_i = \sigma_{\min} + \Delta(i-1)$, with $\Delta = (\sigma_{\max} - \sigma_{\min})/(N-1)$. Note that $\sigma_{\max}/\sigma_{\min} \rightarrow \infty$ at $\delta_{\infty} = 1/\sqrt{3}$.

The numerical investigation of equilibrium properties

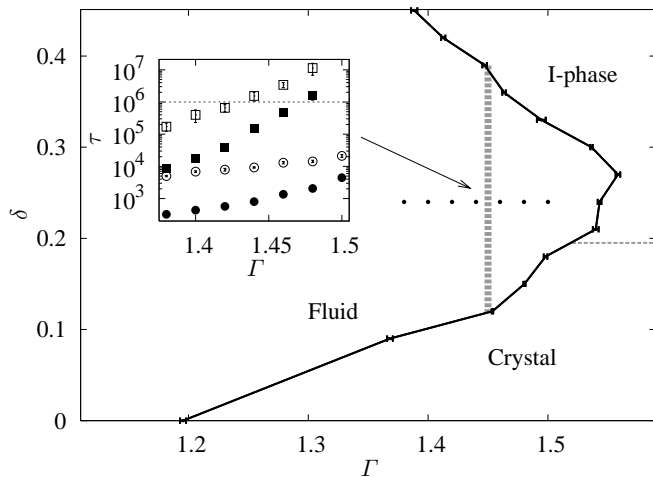


FIG. 1: The $\Gamma - \delta$ phase diagram shows three phases: a fluid at high temperatures, a crystal, and a inhomogeneous solid (I-phase). The boundary between the crystal and the I-phase lies at $0.18 < \delta_c < 0.21$. The vertical line in the fluid phase is the kinetic glass transition. (*Inset*) Integrated relaxation time [12], τ , for e (full) and \mathcal{F} (open), both for standard (squares) and local swap (circles) MC, for $N = 256$. The kinetic glass transition arises when $\tau \sim 10^6$ standard MC steps.

of fluids is limited by the practical impossibility to equilibrate when either the relaxation time τ within the fluid phase, or the freezing time t_{fr} [31] become comparable with the time scale of the simulation. In order to achieve equilibrium we straightforwardly adapt to model (1) the local swap MC algorithm [12, 13], which outperforms [13, 14] other algorithms, such as the non-local swap MC [15] and the density of states MC [16]. In fact, the standard method of studying a first-order transition in a system of finite size, L , looks for a double peak in the histogram of the internal energy per particle e , accompanied by a peak of the specific heat C_V [17, 18]. This procedure is extremely demanding on the quality of the statistical sampling, and has been scarcely used (if at all) for glass-forming liquids or colloids. Fortunately, the local swap MC allows us to employ it.

The thermalization issue needs to be addressed in three different regimes, see Fig. 1: the liquid phase, at the phase coexistence line, and the solid phase. The swap algorithm avoids the cage effect, thus equilibrating easily the whole liquid phase (it reduces τ by two orders of magnitude as compared with standard MC, see Fig. 1–inset). Thermalization in the deep solid phase, not attempted in this work, would require a different approach. At the phase coexistence line, our criterion for thermalization required the observation of tenths of back and forth tunneling events between the liquid and solid phase. The difficulty for meeting the criterion grows dramatically with the number of particles ($\sim \exp[\Sigma N^{2/3}]$, Σ being the liquid-solid surface tension). A stronger, more quantitative check is the consistency of the histogram reweighting [32]. We equilibrated $N = 256$ particles for $\delta \geq 0.1$ (and for the monodisperse system) and $N = 500$

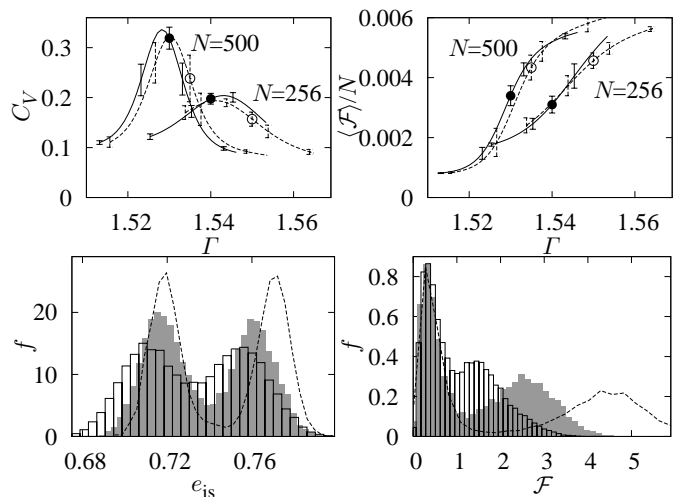


FIG. 2: Equilibrium quantities for $\delta = 0.24$ (*top-left*) Specific heat vs. Γ , from two simulations, one at the size dependent critical point (full symbols denote the actual simulations, full lines coming from histogram reweighting), the other at a higher Γ (open symbols, and dashed lines). The maximum of the specific heat scales with N . (*Top-right*) $\langle \mathcal{F} \rangle / N$ vs. Γ for the same simulations of top-left panel. (*Bottom-left*) Normalized histogram, f , of the energy of the inherent structures, for $N = 256$ (empty) and $N = 500$ (filled), at the Γ value where the peaks of the instantaneous energy have equal height [18]. Inherent structures were found every 10^5 MC steps. (*Bottom-right*) As Bottom-left, for \mathcal{F} . In the fluid phase \mathcal{F} is $\mathcal{O}(1)$ (in the solid, \mathcal{F} is $\mathcal{O}(N)$). We also show (dashed line) e_{is} and \mathcal{F} histograms for $N = 864$, where only two back and forth tunneling events between the liquid and solid phase were observed. Yet, data nicely agree with the predicted N -scaling.

for $\delta \geq 0.21$. However, for local swap MC t_{fr} remains between 10^6 and 10^7 MC steps for all δ , while for standard MC it grows beyond 10^9 steps for $\delta > 0.12$.

To detect the possible existence of large density fluctuations we focus on $\mathcal{S}(\mathbf{q}) \equiv \frac{1}{N} \sum_{i,j} \exp[i\mathbf{q} \cdot (\mathbf{r}_i - \mathbf{r}_j)]$ (\mathbf{r}_i is the position of the i -th particle). Note that $\langle \mathcal{S}(\mathbf{q}) \rangle$ is the static structure factor. The longest wavelengths fluctuations are studied through $\mathcal{F} \equiv [\mathcal{S}(\frac{2\pi}{L}, 0, 0) + \mathcal{S}(0, \frac{2\pi}{L}, 0) + \mathcal{S}(0, 0, \frac{2\pi}{L})]/3$. In fact, in an homogeneous liquid or crystal phase we expect \mathcal{F} to be of order 1, but for a macroscopically inhomogeneous phase it becomes of order N .

In Fig. 2 we show as an example the results obtained for $\delta = 0.24$ where an evidence for a freezing transition is presented. The specific-heat displays a peak of height proportional to N while, as usual for small systems, its position suffers a strong finite size shift. We found convenient to use the histogram of the energy per particle of the inherent structures e_{is} , i.e. the minima of the potential energy [19]. The advantages are twofold (Fig. 2): it largely absorbs the effects of the finite-system shift of the critical temperature (so that the position of the peaks is almost N independent) and it makes each peak narrower.

Note that $\delta = 0.24$ is much higher than the terminal polydispersity δ_t reported in experiments and simulations [7, 11]. Actually, a freezing transition arises in the

full range of δ studied. The line of phase-coexistence, as located by the arising of a double peak for $N = 256$, between the fluid and the solid phase is shown in Fig. 1.

For $\delta=0$, we find a body-centered cubic (bcc) crystal, as expected for modest N [20]. Indeed, $\mathcal{S}(\mathbf{q})$ displays peaks of order N at $\mathbf{q} \sim \frac{2\pi}{a}(1, 1, 0)$, $\frac{2\pi}{a}(0, 1, 1)$, $\frac{2\pi}{a}(1, 0, 1)$ with lattice spacing $a \sim 0.78$. The same Bragg peaks are found at $\delta=0.12$, broadened due to disorder [33] (as compared with $\delta=0$, the intensity reduces by a factor $1/4$, but it still increases linearly with N).

Interestingly, for $\delta=0.24$ the histogram of \mathcal{F} (Fig. 2) develops a double peak at the freezing point. Left-peak's position is N -independent, as expected for the liquid phase (see also the scatter plot in Fig. 3). On the other hand, the second peak (corresponding to the solid) shifts right proportionally to N , revealing that the solid phase is not a standard crystalline one. For $N=500$ and $\delta \lesssim 0.2$ it is risky to use histogram techniques, as the tunneling from solid to liquid is harder to observe than the reverse liquid to solid tunneling, thus we show in Fig. 3 a scatter plot. It is clear that in the crystals we found at $\delta=0.18$ (corresponding to the lower values of e_{IS} in Fig. 3) \mathcal{F} takes a N -independent value [34]. Summarizing, at high polydispersities we have found a freezing transition from the liquid to a solid inhomogeneous phase, while at low polydispersities the low temperature high density phase (large Γ 's) is a standard homogeneous crystal. The study of the transition between the crystal and the I-phase is left for future work. To gain some insight about the I-phase we measured the intensity of the Bragg peaks for the inherent structures in the solid phase. More precisely, we define \mathcal{B} as the maximum [35] of $\mathcal{S}(\mathbf{q})$. In a crystal \mathcal{B} is of order N (the corresponding \mathbf{q} is in the reciprocal lattice), while in a fluid \mathcal{B} is always of order 1. In Fig. 4 we show the histogram of \mathcal{B} along the phase coexistence line both for $N=256$ and $N=500$. For every δ we find a double peak structure. The solid's peak shifts right proportionally N . Thus $\langle \mathcal{B} \rangle$ and $\langle \mathcal{F} \rangle$ provide a classification of the $\Gamma - \delta$ plane: $\langle \mathcal{B} \rangle$ distinguishes the solid from the fluid phase, while $\langle \mathcal{F} \rangle$ is of order N only in the I-phase.

The solid peak in Fig. 4 shifts left with increasing δ (at $\delta=0.45$ the two peaks are hardly resolved). The I-phase might signal either fractionation [4, 5] or phase coexistence of a crystal with an amorphous solid (Fig. 4, top-left). Further work is needed to clarify this point.

The existence of a freezing transition for all δ rules out the terminal polydispersity scenario. But even if a stable solid phase exists for large δ , it might be *dynamically* inaccessible on experimental time-scales. In order to detect the occurrence of the kinetic glass transition on the $\delta - \Gamma$ plane we adopted standard MC simulations which (at variance with local swap MC), mimic the real dynamics of the system by modeling it as a Brownian motion. Note that the correspondence between the single step of standard MC and the physical time units widely differ for liquids and colloids, being $\sim 10^{-13}$ secs. in the former

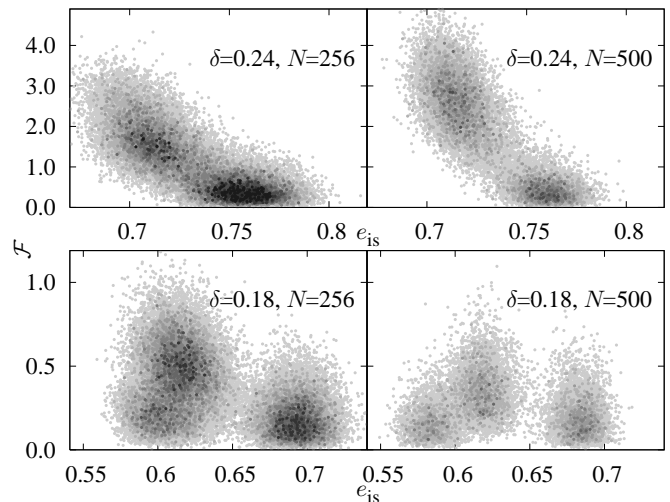


FIG. 3: Scatter plot of \mathcal{F} vs. e_{IS} below (bottom) and above (top) the I-phase-crystal transition line at the liquid-solid phase coexistence, for $N=256$ (left) and $N=500$ (right). The number of points is ~ 45000 ($N=256$) or ~ 15000 ($N=500$). The darker the shade of gray, the higher the density of points.

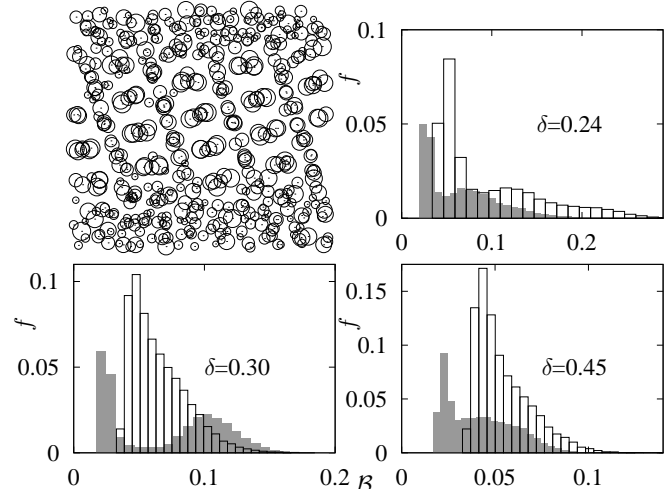


FIG. 4: (Top-left) A $\delta = 0.3$ solid configuration of 500 particles, at phase coexistence, as projected into the XY plane (circles are centered at particles positions, their diameter being proportional to particle sizes). Larger particles form the crystalline central band (the Bragg peaks's analysis suggests a FCC ordering). Normalized histograms of \mathcal{B} for $\delta=0.24, 0.3, 0.45$ with 256 (empty) and 500 (filled) particles.

case and $\sim 10^{-2}$ secs. in the latter one [21].

We have located the kinetic glass transition in Fig. 1 as the point where τ reaches 10^6 (standard) MC steps. In the case of colloids, this roughly corresponds to a relaxation time of three hours, hence our kinetic glass transition corresponds to the experimental one. On the other hand, since in the case of liquids 10^6 MC steps $\sim 10^{-7}$ secs., our kinetic glass transition is rather close to the mode-coupling transition [22]. Indeed, for most molecular and polymeric glass-formers τ at the mode-coupling transition lies between $10^{-7.5}$ and $10^{-6.5}$ secs. [23]. By the way, since τ grows by many order of magnitudes in

a narrow range, for liquids the difference in Γ between the experimental and the mode coupling transition will not be larger than 5% [24]. In the inset of Fig. 1 we observe that the kinetic glass transition is at $\Gamma_c \simeq 1.45$ for $\delta=0.24$. This value coincides with the one found for the soft-spheres binary mixtures (i.e. a bimodal $P(\sigma)$) with $\delta=0.09$ [25] and $\delta=0.16$ [26]. This suggests that Γ_c is independent on δ . The vertical line at $\Gamma_c=1.45$ intersects the freezing transition line at two *intersection points*, creating a sort of no man's land where equilibrium is experimentally unreachable on human time-scales. In fact, the freezing time t_{fr} depends on δ , growing tremendously along the phase coexistence line. When approaching the first intersection point ($\delta \approx 0.12$, see Fig. 1), for standard MC we only know that t_{fr} becomes larger than 10^9 steps. For $\delta > 0.12$ our standard MC simulations did not find the solid phase. We thus argue that the tremendous slowing down both of τ and t_{fr} makes the solid phase for $\delta \gtrsim 0.12$ experimentally unattainable.

We studied the equilibrium phase diagram in the $\delta - \Gamma$ plane for a polydisperse soft sphere model with emphasis on the first order freezing transition. Optimized MC algorithms and Finite Size Scaling analysis were crucial to obtain equilibrium properties. We found two different solid phases, a standard crystal at small δ and a highly inhomogeneous phase at large δ . Moreover, for δ lying between 0.12 and 0.38 the glass transition is no longer preempted by the freezing transition, making this range very promising for the theoretical study of glasses. In experiments non-equilibrium effects should dominate the whole region $\delta \gtrsim 0.12$, where either the kinetic glass transitions or the growth of the freezing time-scale are expected to hide the freezing transition. This is in quantitative agreement with the findings for colloids [7] suggesting that the polydisperse soft-spheres model (1) could catch the features both of molecular glass-formers and of colloids.

We thank V. Erokhin and F. Zamponi for discussions. We were supported by MEC (Spain), through contracts BFM2003-08532, FIS2004-05073, FPA2004-02602 and by BSCH—UCM. The CPU time utilized (at BIFI and CINECA) amounts to 10 years of 3 GHz PentiumIV.

versity Press, 1997).

-
- [1] F. Sciortino and P. Tartaglia, *Adv. Phys.* **54**, 471 (2005).
 - [2] M. Fasolo and P. Sollich, *Phys. Rev. E* **70**, 041410 (2004).
 - [3] P. Chaudhuri, S. Karmakar, C. Dasgupta, H. R. Krishnamurthy, and A. K. Sood, *Phys. Rev. Lett.* **95**, 248301 (pages 4) (2005).
 - [4] P. Bartlett, *J. Chem. Phys.* **109**, 10970 (1998).
 - [5] D. A. Kofke and P. G. Bolhuis, *Phys. Rev. E* **59**, 618 (1999).
 - [6] S. Auer and D. Frenkel, *Nature* **413**, 711 (2001).
 - [7] P. N. Pusey and W. van Megen, *Nature* **320**, 340 (1986).
 - [8] R. P. A. Dullens and W. K. Kegel, *Phys. Rev. Lett.* **92**, 195702 (pages 4) (2004).
 - [9] P. G. Debenedetti, *Metastable Liquids* (Princeton University Press, 1997).
 - [10] J. P. Hansen and I. R. McDonald, *Theory of Simple Liquids* (Academic Press, San Diego, 1986).
 - [11] L. Santen and W. Krauth, *condmat/0107459* (2001).
 - [12] L. A. Fernández, V. Martín-Mayor, and P. Verrocchio, *Phys. Rev. E* **73**, 020501(R) (2006).
 - [13] L. A. Fernández, V. Martín-Mayor, and P. Verrocchio, *Philosophical Magazine* **87**, 581 (2006).
 - [14] L. A. Fernández, V. Martín-Mayor, and P. Verrocchio (AIP, Melville, New York, 2005), no. 832 in *AIP Conference Proceedings Series*, pp. 128–133.
 - [15] T. S. Grigera and G. Parisi, *Phys. Rev. E* **63**, 045102(R) (2001).
 - [16] Q. Yan, T. S. Jain, and J. J. de Pablo, *Phys. Rev. Lett.* **92**, 235701 (pages 4) (2004).
 - [17] M. S. S. Challa, D. P. Landau, and K. Binder, *Phys. Rev. B* **34**, 1841 (1986).
 - [18] J. Lee and J. M. Kosterlitz, *Phys. Rev. Lett.* **65**, 137 (1990).
 - [19] F. H. Stillinger and T. A. Weber, *Phys. Rev. A* **28**, 2408 (1983).
 - [20] P. R. ten Wolde, M. J. Ruiz-Montero, and D. Frenkel, *Phys. Rev. Lett.* **75**, 2714 (1995).
 - [21] N. B. Simeonova and W. K. Kegel, *Phys. Rev. Lett.* **93**, 035701 (pages 4) (2004).
 - [22] W. Götze and L. Sjögren, *Rep. Prog. Phys.* **55**, 241 (1992).
 - [23] V. N. Novikov and A. P. Sokolov, *Phys. Rev. E* **67**, 031507 (pages 6) (2003).
 - [24] E. Rössler, A. P. Sokolov, A. Kisliuk, and D. Quitmann, *Phys. Rev. B* **49**, 14967 (1994).
 - [25] B. Bernu, J. P. Hansen, Y. Hiwatari, and G. Pastore, *Phys. Rev. A* **36**, 4891 (1987).
 - [26] C. C. Yu and H. M. Carruzzo, *Phys. Rev. E* **69**, 051201 (2004).
 - [27] M. Falcioni, E. Marinari, M. L. Paciello, G. Parisi, and B. Taglienti, *Phys. Lett. B* **108**, 331 (1982).
 - [28] A. M. Ferrenberg and R. H. Swendsen, *Phys. Rev. Lett.* **63**, 1195 (1989).
 - [29] H. J. Schöpe, G. Bryant, and W. van Megen, *Phys. Rev. Lett.* **96**, 175701 (pages 4) (2006).
 - [30] We use the long distance cut-off of [13, 16]. Our length unit σ_0 is fixed by $\sigma_0^3 = \int d\sigma_i d\sigma_j P(\sigma_i)P(\sigma_j)(\sigma_i + \sigma_j)^3$. We simulated N (initially fully disordered) particles in a box with periodic boundary conditions at $\rho = \sigma_0^{-3}$.
 - [31] We define t_{fr} as the characteristic time for the first tunneling from the liquid to the solid phase.
 - [32] The average for a N particles system at temperature $1/(\beta + \delta\beta)$, of any function $A[\{x_i\}]$, can be obtained [27, 28] from mean-values at temperature $1/\beta$ through the identity $\langle A \rangle_{\beta + \delta\beta} = \langle A \exp[-N\delta\beta e] \rangle_{\beta} / \langle \exp[-N\delta\beta e] \rangle_{\beta}$, (e is the energy per particle), that, in the $\delta\beta \rightarrow 0$ limit, yields the (differential) Fluctuation-Dissipation Theorem $\partial_{\beta} \langle A \rangle_{\beta} = N[\langle A e \rangle_{\beta} - \langle A \rangle_{\beta} \langle e \rangle_{\beta}]$. Thus, the reweighting method exploits an (integral) Fluctuation-Dissipation Theorem, and consistency in the extrapolation (in practice, $\delta\beta \lesssim [NC_V]^{-1/2}$) is a strong thermalization test.
 - [33] See [29] for recent experiments at low polydispersity.
 - [34] The e_{IS} dispersion at $\delta=0.18$ crystals in Fig. 3 is due to the interplay between spatial orientation and periodic boundary conditions.
 - [35] Maximum over $\mathbf{q} = \frac{2\pi}{L}(n_1, n_2, n_3)$, $|n_i| \leq 20$ and $\mathbf{q} \neq 0$.